Imaging of Soft-Tissue Tumors Using L-3-[Iodine-123]Iodo-α-methyl-tyrosine Single Photon Emission Computed Tomography: Comparison with Proliferative and Mitotic Activity, Cellularity, and Vascularity[1]

Pieter L. Jager,[2] Boudewijn E. C. Plaat, Elisabeth G. E. de Vries, Willemina M. Molenaar, Willem Vaalburg, D. Albertus Piers, and Harald J. Hoekstra

Departments of Nuclear Medicine [P. L. J., D. A. P.], Pathology [B. E. C. P., W. M. M.], Medical Oncology [E. G. E. d. V.], Surgical Oncology [H. J. H.], and Positron Emission Tomography Center [W. V.], University Hospital Groningen, 9700 RB Groningen, the Netherlands

ABSTRACT

The radiolabeled amino acid L-3-[^{123}I]-iodo-α-methyl-tyrosine (IMT) is a new tumor tracer that accumulates in many tumors and is suitable for single photon emission computed tomography (SPECT) imaging. Using IMT SPECT, we studied 32 patients with a soft-tissue tumor suspected to be a soft-tissue sarcoma to determine whether: (*a*) tumors can be visualized; (*b*) benign and malignant lesions can be distinguished; and (*c*) IMT uptake is related to tumor grade and proliferation. Whole-body imaging was performed 15 min after administration of 300 MBq IMT, biopsy, or resection 1–2 weeks later. IMT uptake was quantified using a region-of-interest method resulting in tumor:background (T:B) ratios. These were compared with tumor grade, mitotic index, tumor cellularity, vascularity, and the Ki-67 proliferation index. Eleven patients had a benign tumor, and 21 patients had a soft-tissue sarcoma. Six benign tumors demonstrated minor IMT uptake, and five lipomas had no uptake. All malignant tumors had high uptake and were clearly visualized. T:B ratios in malignant tumors (3.83 ± 1.16) were higher ($P < 0.001$) than in benign tumors (1.52 ± 0.60). Small (<5 mm) metastases in two patients were not detected. Taking the T:B ratio 2.0 as the cutoff level, the sensitivity for detection of malignancy was 100%, and specificity was 88%. IMT uptake correlated with histological grade ($r = 0.82$; $P < 0.001$), mitotic index ($r = 0.75$; $P < 0.001$), tumor cellularity ($r = 0.73$; $P < 0.01$), and with the Ki-67 proliferation index ($r = 0.63$; $P < 0.01$). In conclusion, IMT SPECT visualized all soft-tissue sarcomas. Uptake in sarcomas was clearly higher than in benign lesions, yielding 100% sensitivity for detection of malignancy at 88% specificity. Uptake increased with higher tumor grade and higher proliferation rate.

INTRODUCTION

Soft-tissue sarcomas are a heterogeneous group of malignant tumors that can arise from mesenchymal structures at any site of the body. These tumors constitute 1% of all cancers. A large proportion (60%) is located in an extremity. They often reach a large size before a diagnosis is established. They grow locally aggressive, frequently invade surrounding tissues, and often disseminate to distant sites (1). Treatment planning depends on information regarding the presence or absence of metastases, the local situation, and histological parameters. Chest CT[3] is commonly used to screen for pulmonary metastases and magnetic resonance imaging to assess the local situation and resectability. The most important prognostic factor is tumor malignancy grade, *i.e.*, a higher tumor grade, is associated with a worse prognosis (1–4).

Considerable interest exists in noninvasive determination of the malignancy grade of sarcomas (5–9). For this purpose, various nuclear medicine techniques, such as SPECT and more recently PET, using various tracers, have been applied. Radiolabeled amino acids are potentially suitable tracers; because of the increased protein metabolism of malignant tumors, the uptake in malignancy is increased (10). Furthermore, amino acid uptake is less disturbed by uptake in inflammatory tissue than the frequently used tracer FDG (11–15). However, most carbon-11-labeled amino acids are difficult to synthesize and require the infrastructure of PET.

The radiolabeled amino acid IMT is avidly taken up in many tumors (16, 17). The agent has been introduced for imaging of brain tumors where tumor uptake was shown to represent amino acid transport activity, an important step in protein metabolism (18–21). Because at present IMT is the only amino acid tracer suitable for SPECT, imaging with this tracer might combine the specificity of amino acids with the wide availability of SPECT.

Received 9/7/99; revised 1/26/00; accepted 2/9/00.

The costs of publication of this article were defrayed in part by the payment of page charges. This article must therefore be hereby marked *advertisement* in accordance with 18 U.S.C. Section 1734 solely to indicate this fact.

[1] Supported by the University Hospital Groningen, the J. K. de Cock Stichting, Amersham Cygne, and The Dutch Cancer Society Grant 95-1085.

[2] To whom requests for reprints should be addressed, at Department of Nuclear Medicine, University Hospital Groningen, P. O. Box 30001, 9700 RB Groningen, the Netherlands. Phone: 31-50-3613541; Fax: 31-50-3611712; E-mail: p.l.jager@nucl.azg.nl.

[3] The abbreviations used are: CT, computed tomography; SPECT, single photon emission tomography; PET, positron emission tomography; FDG, ^{18}F-fluoro-2-deoxy-D-glucose; IMT, L-3-[^{123}I]iodo-α-methyl-tyrosine; ROI(s), region(s) of interest; T:B, tumor:background.

Table 1 Patient characteristics and IMT uptake

No.	Age	Sex	Tumor histology	Location	Size (cm)	Grade	IMT T:B ratio
Malignant lesions							
1	33	F	Liposarcoma (sclerosing)	Upper leg	10	Low	2.3
2	58	M	Liposarcoma	Retroperitonal	23	Low	2.6
3	32	F	Liposarcoma	Upper leg	6	Low	2.8
4	45	M	Liposarcoma (myxoid)	Lower leg	13	Low	2.9
5	47	F	Liposarcoma (myxoid)	Knee	6	Intermediate	3.8
6	36	M	Malignant fibrous histiocytoma	Abdominal wall	8	Intermediate	3.8
7	82	M	Malignant fibrous histiocytoma	Lower Leg	7	Intermediate	5.4
8	43	M	Sarcoma not otherwise specified	Upper leg	12	Intermediate	4.0
9	35	F	Synovial sarcoma	Upper leg	6	Intermediate	3.2
10	18	M	Extraskeletal osteosarcoma	Chest wall	5	High	2.7
11	29	M	Extraskeletal mesenchymal chondrosarcoma	Elbow	2	High	4.1
12	58	M	Liposarcoma	Chest wall	9	High	5.2
13	46	M	Liposarcoma (pleiomorphic)	Upper leg	20	High	3.6
14	46	F	Malignant fibrous histiocytoma	Upper leg	8	High	5.1
15	75	M	Malignant fibrous histiocytoma	Upper leg	10	High	5.8
16	64	M	Malignant fibrous histiocytoma	Chest wall	6	High	6.1
17	19	M	Malignant schwannoma	Gluteal	7	High	3.2
18	18	F	Sarcoma not otherwise specified	Gluteal	7	High	2.2
19	54	F	Sarcoma not otherwise specified	Knee	10	High	3.5
20	66	M	Sarcoma not otherwise specified	Knee	10	High	4.8
21	52	F	Synovial sarcoma	Lower leg	10	High	3.4
Benign lesions							
22	24	F	Fibromatosis, locally invasive	Neck	5		1.8
23	23	F	Fibromatosis, locally invasive	Chest wall	6		2.5
24	41	M	Intramuscular hemangioma	Back	2		1.5
25	42	F	Intramuscular haemangioma	Lower leg	8		1.8
26	74	F	Lipoma	Axilla	15		1.0
27	52	F	Lipoma	Shoulder	6		1.0
28	56	M	Lipoma	Upper leg	7		1.0
29	53	F	Lipoma	Upper leg	8		1.0
30	42	F	Lipoma	Back	5		1.0
31	28	M	Neurofibroma	Groin	10		2.6
32	58	F	Non specific fibrosis	Upper leg	10		1.5

The goals of this study were to determine whether: (*a*) IMT SPECT can visualize soft-tissue sarcomas; (*b*) IMT uptake can discriminate between benign and malignant tumors; and (*c*) uptake is related to tumor grade and the degree of proliferation, using the mitotic index and the Ki-67 proliferation index as markers.

PATIENTS AND METHODS

Patients. Patients referred to the University Hospital Groningen between October 1997 and February 1999 for management of a suspected soft-tissue sarcoma were asked to participate in this study. Suspicion for malignancy was based on rapid growth, size, consistency at palpation, location, and radiographic appearance of the tumor. Selection criteria included age >18 years and planned histological confirmation within 2 weeks after the IMT study.

Thirty-two patients [16 males and 16 females; median age, 45 years (range, 18–82)] were included in the study. Patient and tumor data are presented in Table 1. All patients were studied 1–2 weeks prior to biopsy or definitive resection. All patients were clinically staged with a chest CT, magnetic resonance imaging, or CT of the soft-tissue mass as well as ultrasound of the liver and bone scintigraphy. The study was approved by the Medical Ethics Committee of the University Hospital Groningen. Written informed consent was obtained from all patients.

Tracer Synthesis. Synthesis of IMT was carried out slightly modified from Krummeich *et al.* (22). Briefly, Iodogen iodination with $Na^{123}I$ [specific activity, >185 TBq/mmol (5000 Ci/mmol); Amersham Cygne, Eindhoven, the Netherlands] of the precursor L-α-methyl-tyrosine was performed in a borate buffer. IMT was purified by elution with saline containing 5% ethanol over a C-18 SepPak cartridge (Waters, Milford, MA) preconditioned with 100% ethanol, followed by saline containing 5% ethanol. After filtration through a sterile 0.22 μm Millex GV filter (Millipore, S. A., Molsheim, France), a colorless ready-to-inject solution was obtained. Samples were demonstrated to be sterile and pyrogen free. Quality control was performed by high-performance liquid chromatography on a RP-18 column (Multosorb 100 4.6) using H_2O:ethanol:acetic acid (87.5:10:2.5, v/v/v %) as eluent. Radiochemical purity was >99% in all cases. The overall synthesis time, including purification and quality control, was <1 h. Radiochemical yield was 50–65%.

Imaging. Patients were injected i.v. with 200–300 MBq IMT after at least a 4-h fast. They were given 10 drops of Lugol's solution p.o. 15 min before injection to prevent thyroid uptake of possibly formed free ^{123}I. A large-field-of-view, double-headed gamma camera (MULTISPECT 2; Siemens, Inc., Hoffman Estates, IL) was used with a medium-energy, all-purpose collimator and a 15% window centered on the 159 kV

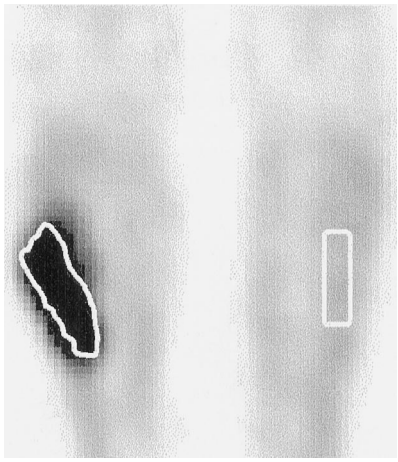

Fig. 1 Coronal SPECT slice through the lower legs and knees of patient 4 with a low-grade myxoid liposarcoma showing a ROI through the tumor drawn at 80% of the maximum count value in the tumor and a contralateral background region.

photopeak of ^{123}I. System resolution was 12 mm full-width at half-maximum at 10-cm distance.

Fifteen min after injection, SPECT imaging of the tumor area was performed, usually followed by a planar spot view. After imaging the tumor area, additional spot views were recorded to obtain whole-body information. In 20 patients, the thorax was additionally imaged using SPECT.

All SPECT acquisitions included 64 views (2 × 32; 5.6°/step) of 30 s duration each in a 128 × 128 matrix format with a zoom factor of 1.23. This corresponds to a pixel dimension of 4.1 mm. Transaxial tomograms were reconstructed without prefiltering using filtered back-projection with a Butterworth filter of sixth order and a cutoff frequency of 0.275 Nyquist. Ten-min spot views were recorded in a 128 × 128 matrix. Total imaging time was ~1 h. The reported radiation burden of IMT is 0.007 mSv/MBq, yielding an effective dose equivalent of 1.4–2.1 mSv (23).

Image Analysis. Without knowledge of the staging and histopathological data, two experienced readers analyzed all images visually for tumor uptake and abnormal extratumoral uptake. ROIs were manually placed over SPECT tumor slices with maximum visibility and on planar spot views. Reference ROIs were placed over representative background muscle tissue, usually contralaterally. ROIs were drawn at 80% of the maximal pixel value around the lesion under study; in some cases, this procedure resulted in more than one ROI per tumor (24). An example is presented in Fig. 1. The T:B ratio was calculated by dividing uptake intensity (counts/pixel) in the tumor ROI by uptake intensity in the background ROI.

All IMT scintigraphic findings were compared with the results of conventional imaging. T:B ratios were compared with tumor grade, mitotic index, tumor cellularity, and vascularity and the Ki-67 proliferation index.

Pathological Examination. The histological diagnosis was made on H&E-stained paraffin sections with or without additional immunohistological stains. All tumors were classified according to Enzinger and Weiss (1) into 10 different histological types. Soft-tissue sarcomas were graded according to the grading system of Coindre *et al.* (25), in which points are assigned to differentiation level, mitotic index, and necrosis.

In 27 of the 32 lesions, determination of the mitotic index, Ki-67 proliferation index, cellularity, and vascularity was performed. In the five remaining cases (three benign and two malignant), there was not enough material left for these determinations. The number of mitotic figures per 2 mm^2 was counted in H&E-stained paraffin sections. Proliferating cells were detected using the monoclonal antibody MIB-1 (Immunotech S. A., Marseille, France), which recognizes an epitope of the Ki-67 antigen. This is a nuclear antigen present in all phases of the cell cycle, except for the G_0 phase, in which the cells are withdrawn from the cell cycle, and the early G_1 phase, the phase before the start of DNA synthesis (26). Immunohistochemistry was performed on paraffin sections according to a method modified from Shi *et al.* (27) and Emanuels *et al.* (28). In brief, after heating on a hot plate, the slides were dewaxed in xylene and rehydrated in serial ethanol washes (100, 96, and 70%). After heating twice in an autoclave for 10 min at 110°C in boiling solution (pH 6.0), the slides were incubated with a 1:400 dilution of the antibody in BSA (pH 7.4). The primary antibody was detected with a biotinylated secondary antibody (multilink), followed by a streptavidin-alkaline phosphatase conjugate (Ready-to-Use Link and Label; Biogenex, San Ramon, CA). Final color was developed using bromochloroindolyl-phosphate 4-nitroblue-tetrazolium chloride (Boehringer Mannheim, Mannheim, Germany).

To measure the Ki-67 proliferation index and tumor cellularity, we used ocular micrometry on a Leica microscope (Rijswijk, the Netherlands) with an eyepiece grid at ×400. Fifteen fields were randomly selected throughout histologically viable areas. Tumor cellularity (cellular density) was defined as the total number of cells excluding endothelial cells, inflammatory cells, and necrosis and presented as number per 2 mm^2. MIB-1-positive nuclei were identified, and the number of these nuclei was divided by the total number of nuclei in each of the 15 fields to calculate an index/field. The Ki-67 proliferation index (also named Ki-67 labeling index), representing proliferative activity, was defined as the mean of the indices of the 15 fields. Vascularity in each tumor was estimated by quantification of the total number of small blood vessels or parts of large vessels in H&E-stained paraffin sections. Ten fields were randomly selected, and the total number of vessels in 10 fields at ×400 (corresponding to 2 mm^2) was counted.

Statistics. To determine the ability to distinguish malignant from benign tumors, a Student's *t* test was performed on T:B ratios (normally distributed) in both groups. Spearman's correlation coefficient was used to correlate T:B ratios with Ki-67 proliferation index, mitotic index, tumor vascularity, and cellularity. Kruskal Wallis nonparametric ANOVA with Dunnett's T3 post-hoc multiple comparisons test was performed to relate tumor grade with T:B ratios. Two-tailed *P*s < 0.05 were considered significant.

RESULTS

Eleven patients were found to have benign lesions; the remaining 21 had soft-tissue sarcomas. Three patients had been treated previously for a soft-tissue sarcoma (2, 3, and 4 years

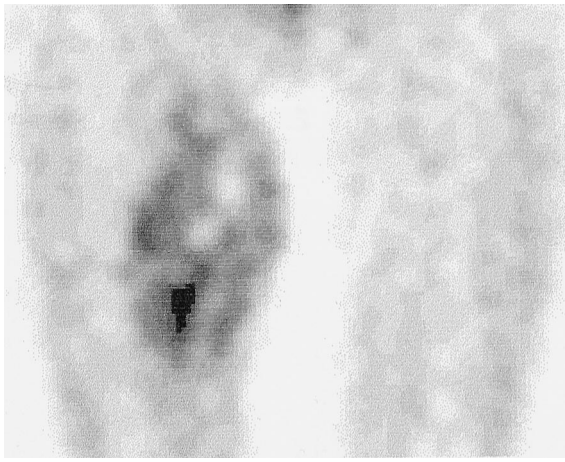

Fig. 2 Coronal SPECT slice through the upper legs of patient 13 with a high-grade liposarcoma showing intense uptake of IMT. Heterogeneous uptake with a central defect is caused by necrosis.

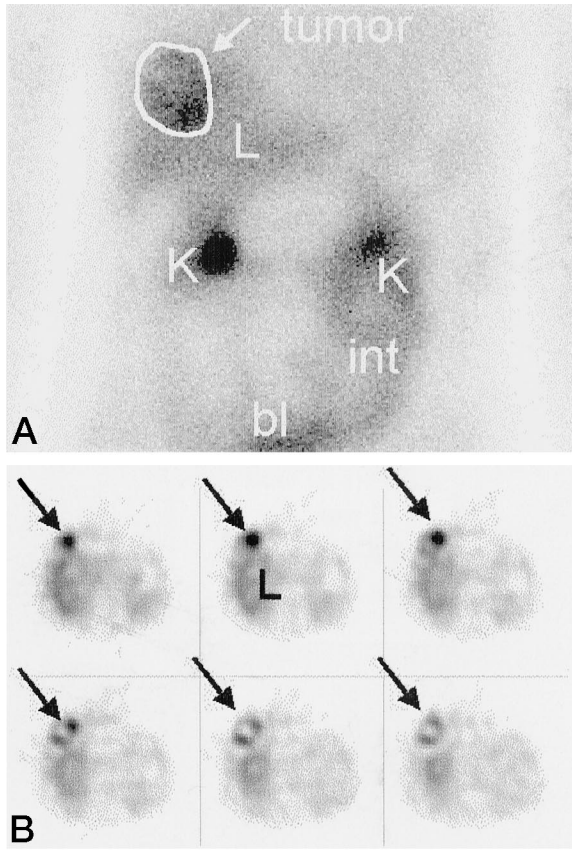

Fig. 3 *A*, planar anterior image of the abdomen of patient 12 with a liposarcoma of the chest wall showing heterogeneous IMT uptake in a lesion that projects over the liver (*circle* and *arrow*). Physiological IMT uptake is present in the liver (*L*), both kidneys and pyela (*K*), intestine (*int*), and bladder (*bl*). *B*, transverse SPECT slices through the liver region (from cranial *upper left* to caudal *lower right*) better demonstrate the localization of the tumor (*arrows*) ventral of the liver (*L*), increased contrast and a central defect, presumably caused by tumor necrosis.

earlier) and were now diagnosed to have a local recurrency. Eighteen tumors were localized in an extremity (56%), and 14 in the trunk (44%). Tumor size was between 2 and 23 cm (median, 8.6 cm). There were 4 low-grade (grade I), 5 intermediate-grade (grade II), and 12 high-grade (grade III) sarcomas (Table 1). Benign lesions were assigned grade 0.

All 21 soft-tissue sarcomas were visualized on the IMT SPECT images. Tumors in the extremities and in the chest were well visualized because of high tumor uptake and low background uptake, whereas tumors near excretory systems (kidneys, bladder, and ureters) were more difficult to evaluate. IMT uptake in tumors was often inhomogeneous, in accordance with the typical histological appearance of sarcomas where areas of necrosis and hemorrhage are interspersed with areas containing vital tumor cells. Typical examples are presented in Figs. 2 and 3.

In 5 of the 11 benign lesions no IMT uptake was found; in four, faint uptake was found, and in two, avid uptake. No uptake was found in all five lipomas, and faint uptake in two large intramuscular hemangiomas, in an aspecific fibrotic lesion, and in an aggressive fibromatosis lesion. Avid uptake was present in a growing neurofibroma and in another aggressive fibromatosis lesion (the latter is considered "borderline malignant").

The average T:B ratio in benign tumors was 1.52 ± 0.60, whereas IMT uptake in the malignant tumors was much higher: 3.83 ± 1.16 ($P < 0.001$; Fig. 4). There was minimal overlap in individual values, attributable to avid uptake in the aggressive fibromatosis and in the growing neurofibroma (Fig. 4). When a T:B ratio of 2.0 was chosen as the cutoff point, sensitivity for the detection of malignancy in a soft-tissue mass was 100% with a specificity of 88%. Using 2.7 as the cutoff point, sensitivity was 89%, but specificity was 100%.

T:B ratios correlated with histological grades ($r = 0.82$; $P < 0.001$); IMT uptake increased with higher tumor grade. Post-hoc analysis revealed that the difference between benign tumors *versus* grade 1, 2, and 3 tumors caused the significance. Grade 1 *versus* grade 2 and grade 2 *versus* grade 3 could not be distinguished from each other. However, low-grade tumors could be discriminated from benign tumors in this group (Fig. 5). In addition, benign and grade 1 tumors together had lower IMT uptake than grade 2 and 3 tumors together ($P < 0.0001$).

Interestingly, IMT uptake correlated with markers of cell proliferation; IMT T:B ratio *versus* the Ki-67 proliferation index gave $r = 0.75$, $P < 0.001$ (Fig. 6*A*) and *versus* the mitotic index $r = 0.63$, $P < 0.01$ (Fig. 6*B*). IMT uptake correlated also with tumor cellularity ($r = 0.73$ $P < 0.001$; Fig. 6*C*), whereas no relation with tumor vascularity could be established (Fig. 6*D*).

Because whole-body images were available in all patients, the ability of IMT scintigraphy to detect metastatic disease was also studied. But because of the low number of metastasized tumors, no reliable assessment of staging could be obtained. Only two patients in this series were found to have metastatic disease; one had small pulmonary metastases (2 mm on chest CT) that were negative on the IMT chest SPECT study, and the other patient had multiple small (<5 mm) intra-peritoneal metastases, negative on all preoperative investigations but detected during surgery.

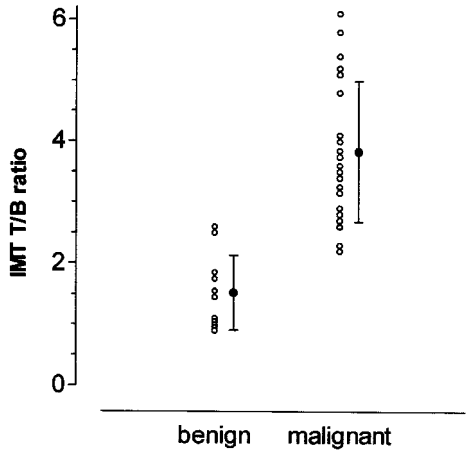

Fig. 4 IMT uptake (T:B ratios) in benign and malignant tumors (○); means; *bars*, SD (●). In malignant lesions, uptake is higher than in benign lesions: 3.83 ± 1.26 *versus* 1.52 ± 0.60, $P < 0.001$.

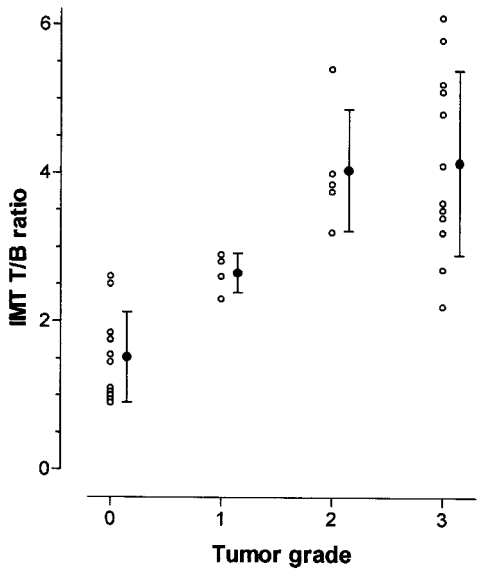

Fig. 5 IMT uptake (T:B ratio) *versus* tumor grade for all tumors (○); means; *bars*, SD (●). Benign tumors are assigned grade 0. Spearman correlation coefficient $r = 0.82$, $P < 0.001$.

DISCUSSION

This study demonstrates high uptake of IMT in soft-tissue sarcomas and low uptake in benign processes. All malignant tumors were visualized, leading to 100% sensitivity. Tumors in the direct vicinity of bladder or kidneys were somewhat more difficult to assess because of renal excretion of IMT causing high background activity. IMT uptake could differentiate benign from malignant tumors with high accuracy. Uptake increased with higher tumor grade, higher Ki-67 proliferation index, mitotic activity, and tumor cellularity, whereas no correlation with tumor vascularity was found. Therefore, this relatively simple noninvasive technique provides information on parameters of tumor activity.

To understand what processes are visualized by IMT uptake, it is important to know the mechanism of uptake. Using competition experiments *in vivo*, Langen *et al.* (19) demonstrated that IMT is a substrate for the amino acid transport systems in the blood-brain barrier. This has not been demonstrated for tumors outside the brain yet. However, *in vitro* data suggest that also in non-glioma tissue, uptake of IMT is almost entirely mediated by amino acid transport activity (29). Because in the present study no correlation with the amount of tumor vessels was found, tumor perfusion is not the dominating factor that governs IMT uptake, as was suggested by Deehan *et al.* (30) in a rat model. One could argue that uptake in the two hemangiomas must be related to blood flow and diffusion, but these tumors were also very cellular. The presumed mechanism of uptake of IMT is the accelerated protein metabolism and the resulting increased demand for amino acids. This is further supported by the relation with tumor proliferation factors, as found in this study.

To noninvasively determine the malignancy grade in soft-tissue tumors, magnetic resonance spectroscopy (9) and various nuclear medicine techniques and tracers have been used, such as ^{201}Tl, ^{99m}Tc-MIBI, ^{99m}Tc-MDP, and ^{67}Ga (31, 32), and more recently FDG and radiolabeled amino acids, such as L-[1-^{11}C]tyrosine (6, 7, 33, 34). Different biochemical processes in tumors are visualized by all these tracers; most likely ^{201}Tl uptake is related to cellular Na^+K^+-ATPase activity, ^{99m}Tc-MIBI to membrane functions and mitochondrial integrity, MDP to calcium/phosphate metabolism, and ^{67}Ga to transferrin receptors in tumor cells or inflammatory cells. In all cases, there is more or less effect of tumor vascularization. Sensitivity of tumor detection using IMT appears better than other single photon tracers in soft-tissue sarcomas, and the presumed uptake mechanism might more directly reflect tumor viability than the above-mentioned mechanisms, but our results need to be confirmed by other studies.

Many studies have used PET to study sarcomas. FDG generally shows high uptake in tumors and has proven to be of value in the visualization and grading of soft-tissue sarcomas. In the study by Nieweg *et al.* (6), all 18 sarcomas were visualized using FDG PET and a correlation was found between the calculated glucose consumption and tumor grade. Schulte *et al.* (8) found high sensitivity using FDG PET for the detection of malignancy in 102 patients, but lower specificity caused by high uptake in aggressive benign tumors and in a patient with myositis ossificans. Uptake of L-1-[^{11}C]tyrosine also showed a correlation with tumor grade, mitotic rate, and proliferation in soft-tissue sarcoma (7, 34). Because of lower uptake in inflammatory reactions caused by radiotherapy, systemic chemotherapy, or regional cytostatic perfusion, it is suggested that radiolabeled amino acids are better suited to monitor treatment effects than FDG (7, 11, 33). The results of the present study using IMT SPECT are well in line with these PET studies, with somewhat higher correlation factors than reported for L-[1-^{11}C]tyrosine (7, 34).

Almost all studies on soft-tissue tumors have found some uptake in benign lesions, regardless of the used tracer (6–8, 31, 32). Also using IMT we found minor uptake in hemangiomas and more avid uptake in a neurofibroma and in aggressive fibromatosis lesions. These latter are actually considered to be

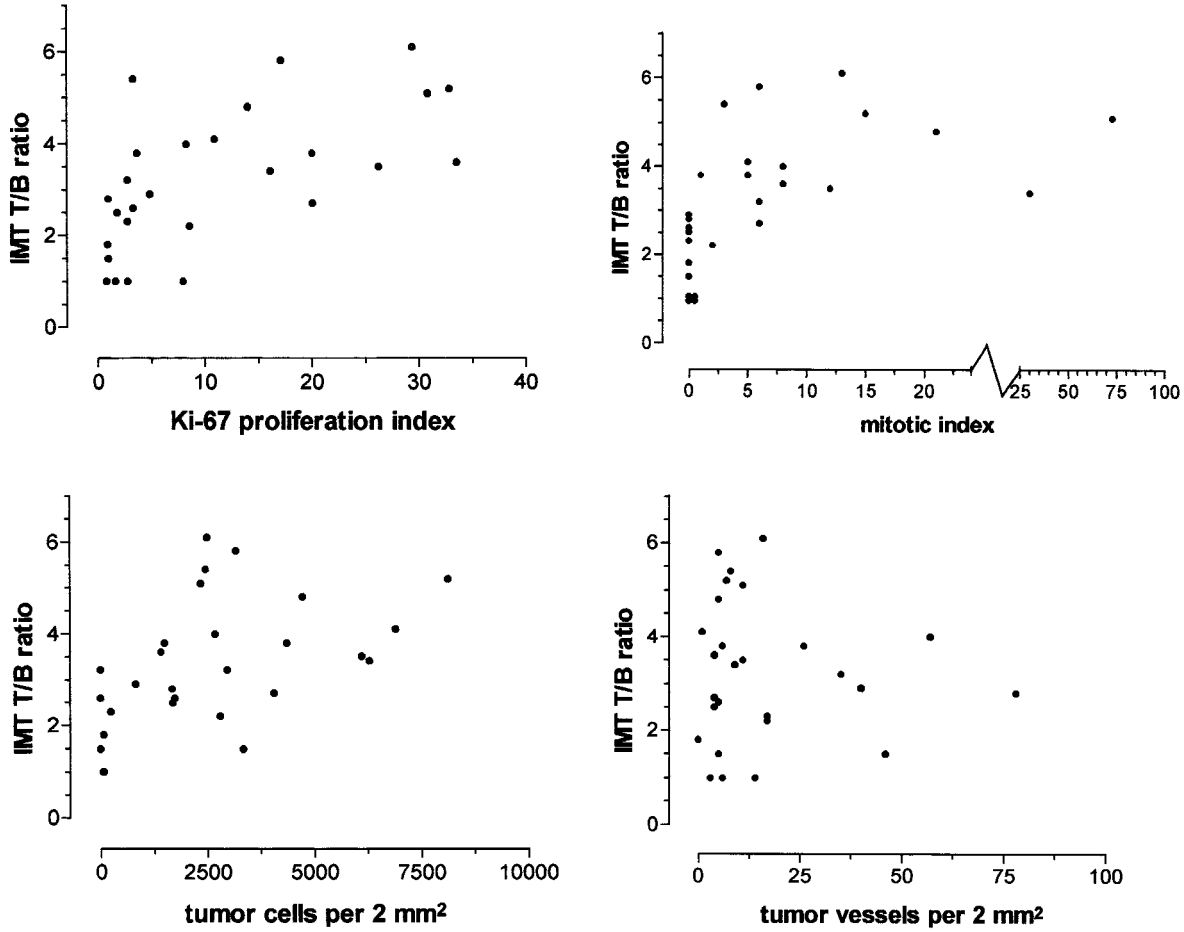

Fig. 6 Scatterplots showing IMT uptake (T:B ratio) in correlation with the Ki-67 proliferation index: $r = 0.63$, $P < 0.01$ (*A*); mitotic index: $r = 0.75$, $P < 0.001$ (*B*); tumor cellularity: $r = 0.73$, $P < 0.001$ (*C*); and tumor vascularity: no correlation (*D*).

"borderline malignant" and therefore presumably have increased amino acid metabolism leading to IMT uptake. Similar to our observations, Kuwert *et al.* (35) found some IMT uptake in nonneoplastic brain lesions such as inflammatory lesions and infarctions. Recently, very high uptake was described in a low-grade desmoplastic infantile ganglioglioma, another benign neoplasm (36). Therefore, it seems most likely to conclude that IMT is an aspecific tumor tracer that targets amino acid metabolism in tumors. Difference in uptake between malignant and benign disease is based on the degree of accelerated protein metabolism.

In this study, we found IMT uptake also to be related with the number of tumor cells. Whether this also holds true for other tracers is largely unknown. Because cellular density can be high in tumors, the mere fact of many cells/volume (in comparison with adjacent tissues) could already cause increased uptake. However, it seems unlikely that this effect only would result in T:B ratios between 3 and 6, as found in many high-grade tumors. Moreover, others have found no relation between IMT uptake and cellular density in brain tumors (37).

The heterogeneity of soft-tissue sarcomas is a frequently occurring difficulty in analyzing the relationship between tracer uptake and histological parameters. This heterogeneity may cause sampling errors in the histological evaluation. In the present study, IMT uptake was based on a standardized ROI analysis encompassing the entire tumor. Histopathological parameters, however, were based on a representative tissue sample obtained from the removed tumor (or large biopsy). Although we tried to reduce sampling errors as much as possible, by analyzing randomly selected microscopic areas within the sample, some degree of sampling error could still be possible. This may influence the significance of the correlations.

Although our results appear comparable with those using FDG and L-[1-^{11}C]tyrosine PET, it could be argued that the lower resolution and limited quantification possibilities of SPECT make the method inferior to PET. However, in these generally large tumors, the lower resolution is presumably not a large problem, although partial volume effects may decrease tumor heterogeneity. Limited quantification possibilities are also controversial, because some authors successfully use T:B ratios also in FDG PET studies (8), whereas others disagree as to what PET uptake parameters give the best results in separation of benign from malignant disease (6, 38–40). Furthermore, absolute quantification of protein synthesis (as possible in PET)

both in tumor tissue and in "background" tissue may be disturbed by systemic influences and vary largely from day to day (33). The use of ratios might compensate for this effect.

The good correlation of IMT uptake with parameters of tumor activity may be of interest in evaluation of new treatment strategies such as angiogenesis inhibition, matrix metalloproteinase inhibition, or antisense therapy. These new drugs exert their action through new mechanisms and may require new evaluation methods. In these methods, assessment of metabolic tumor activity may complement the classic response parameter, the change in tumor size. In current routine clinical practice, however, noninvasive studies of tumor activity or its benign/malignant nature is of limited value. In general, patients and physicians rely on histological evidence, and only in exceptional cases will these studies influence diagnostic or therapeutic strategies, although the good separation between grade 1 *versus* higher grade tumors may assist in determination of the prognosis.

In conclusion, IMT scintigraphy clearly visualized all soft-tissue sarcomas in this group. Uptake in malignant tumors was higher than in benign lesions, leading to a sensitivity for the detection of malignancy of 100% at a specificity of 88%. Uptake increased with higher tumor grade and higher proliferation rate. Therefore, IMT SPECT noninvasively provides information about tumor activity.

REFERENCES

1. Enzinger, F. M., and Weiss, S. W. Soft tissue tumors. St. Louis: C. V. Mosby, 1995.

2. Coindre, J. M., Terrier, P., Bui, N. B., Bonichon, F., Collin, F., Le Doussal, V., Mandard, A. M., Vilain, M. O., Jacquemier, J., Duplay, H., Sastre, X., Barlier, C., Amar, H. M., Lesech, M. J., and Contesso, G. Prognostic factors in adult patients with locally controlled soft tissue sarcoma. A study of 546 patients from the French Federation of Cancer Centers Sarcoma Group. J. Clin. Oncol., *14:* 869–877, 1996.

3. Rossi, C. R., Foletto, M., Alessio, S., Menin, N., D'Amore, E., Rigon, A., and Lise, M. Limb-sparing treatment for soft tissue sarcomas: influence of prognostic factors. J. Surg. Oncol., *63:* 3–8, 1996.

4. Ham, S. J., van der Graaf, W. T., Pras, E., Molenaar, W. M., van den Berg, E., and Hoekstra, H. J. Soft tissue sarcoma of the extremities. A multimodality diagnostic and therapeutic approach. Cancer Treat Rev., *24:* 373–391, 1998.

5. Lamki, L. M. Tissue characterization in nuclear oncology: its time has come. J. Nucl. Med., *36:* 207–210, 1995.

6. Nieweg, O. E., Pruim, J., van Ginkel, R. J., Hoekstra, H. J., Paans, A. M., Molenaar, W. M., Schraffordt Koops, H., and Vaalburg, W. Fluorine-18-fluorodeoxyglucose PET imaging of soft-tissue sarcoma. J. Nucl. Med., *37:* 257–261, 1996.

7. Kole, A. C., Plaat, B. E., Hoekstra, H. J., Vaalburg, W., and Molenaar, W. M. FDG and L-[1–11C]-tyrosine imaging of soft-tissue tumors before and after therapy. J. Nucl. Med., *40:* 381–386, 1999.

8. Schulte, M., Brecht-Krauss, D., Heymer, B., Guhmann, A., Hartwig, E., Sarkar, M. R., Diederichs, C. G., Schultheis, M., Kotzerke, J., and Reske, S. N. Fluorodeoxyglucose positron emission tomography of soft tissue tumours: is a non-invasive determination of biological activity possible? Eur. J. Nucl. Med., *28:* 599–605, 1999.

9. Hoekstra, H. J., Boeve, W. J., Kamman, R. L., and Mooyaart, E. L. Clinical applicability of human *in vivo* localized phosphorus-31 magnetic resonance spectroscopy of bone and soft tissue tumors. Ann. Surg. Oncol., *1:* 504–511, 1994.

10. Isselbacher, K. J. Sugar and amino acid transport by cells in culture–differences between normal and malignant cells. N. Engl. J. Med., *286:* 929–933, 1972.

11. Kubota, K., Matsuzawa, T., Fujiwara, T., Sato, T., Tada, M., Ido, T., and Ishiwata, K. Differential diagnosis of AH109A tumor and inflammation by radioscintigraphy with L-[methyl-^{11}C]-methionine. Jpn. J. Cancer Res., *80:* 778–782, 1989.

12. Kubota, K., Tada, M., Yamada, S., Hori, K., Saito, S., Iwata, R., Sato, K., Fukuda, H., and Ido, T. Comparison of the distribution of fluorine-18 fluoromisonidazole, deoxyglucose and methionine in tumour tissue. Eur. J. Nucl. Med., *26:* 750–757, 1999.

13. Kubota, R., Kubota, K., Yamada, S., Tada, M., Takahashi, T., Iwata, R., and Tamahashi, N. Methionine uptake by tumor tissue: a microautoradiographic comparison with FDG. J. Nucl. Med., *36:* 484–492, 1995.

14. Kole, A. C., Nieweg, O. E., Pruim, J., Paans, A. M., Plukker, J. T., Hoekstra, H. J., Schraffordt Koops, H., and Vaalburg, W. Standardized uptake value and quantification of metabolism for breast cancer imaging with FDG and L-[1–11C]tyrosine PET. J. Nucl. Med., *38:* 692–696, 1997.

15. Strauss, L. G. Fluorine-18-deoxyglucose and false-positive results: a major problem in the diagnostics of oncological patients. Eur. J. Nucl. Med., *23:* 1409–1415, 1996.

16. Jager, P. L., Franssen, E. J. F., Kool, W., Szabo, B. G., Hoekstra, H. J., Groen, H. J. M., de Vries, E. G. E., van Imhoff, G. W., Vaalburg, W., and Piers, D. A. Feasibility of tumor imaging using L-3-[^{123}I]iodo-α-methyl-tyrosine in extra-cranial tumors. J. Nucl. Med., *39:* 1736–1743, 1998.

17. Flamen, P., Bernheim, N., Deron, P., Caveliers, V., Chavatte, K., Franken, P. R., and Bossuyt, A. Iodine-123 α-methyl-L-tyrosine single-photon emission tomography for the visualization of head and neck squamous cell carcinomas. Eur. J. Nucl. Med., *25:* 177–181, 1998.

18. Langen, K. J., Coenen, H. H., Roosen. N., Kling, P., Muzik, O., Herzog, H., Kuwert, T., Stocklin, G., and Feinendegen, L. E. SPECT studies of brain tumors with L-3-[^{123}I]iodo-α-methyl-tyrosine: comparison with PET, [^{124}I]IMT and first clinical results. J. Nucl. Med., *31:* 281–286, 1990.

19. Langen, K. J., Roosen, N., Coenen, H. H., Kuikka, J. T., Kuwert, T., Herzog, H., Stocklin, G., and Feinendegen, L. E. Brain and brain tumor uptake of L-3-[^{123}I]iodo-α-methyl-tyrosine: competition with natural L-amino acids. J. Nucl. Med., *32:* 1225–1228, 1991.

20. Oldendorf, W. H. Saturation of amino acid uptake by human brain tumor demonstrated by SPECT. J. Nucl. Med., *32:* 1229–1230, 1991.

21. Kawai, K., Fujibayashi, Y., Saji, H., Yonekura, Y., Konishi, J., Kubodera, A., and Yokoyama, A. A strategy for the study of cerebral amino acid transport using iodine-123-labeled amino acid radiopharmaceutical: 3-iodo-α-methyl-L-tyrosine. J. Nucl. Med., *32:* 819–824, 1991.

22. Krummeich, C., Holschback, M., and Stöcklin, G. Direct n.c.a. electrophilic radioiodination of tyrosine analogues: their *in vivo* stability and brain-uptake in mice. Appl. Radiat. Isot., *45:* 929–935, 1994.

23. Schmidt, D., Langen, K. J., Herzog, H., Wirths, J., Holschbach, M., Kiwit, J. C., Ziemons, K., Coenen, H. H., and Müller-Gärtner, H. Whole body kinetics and dosimetry of L-3-[^{123}I]iodo-α-methyl-tyrosine. Eur. J. Nucl. Med., *24:* 1162–1166, 1997.

24. Kuwert, T., Morgenroth, C., Woesler, B., Matheja, P., Palkovic, S., Vollet, B., Schafers, M., Wassmann, H., and Schober, O. Influence of size of regions of interest on the measurement of uptake of 123I-α-methyl-tyrosine by brain tumors. Nucl. Med. Commun., *17:* 609–615, 1996.

25. Coindre, J. M., Trojani, M., Contesso, G., Rouesse, J., Bui, N. B., Bodaert, A., De Mascarel, I., de Mascarel, A., and Goussot, J. F. Reproducibility of a histopathologic grading system for adult soft tissue sarcoma. Cancer (Phila.), *58:* 306–309, 1986.

26. Gerdes, J., Lemke, H., Baisch, H., Wacker, H. H., Schwab, U., and Stein, H. Cell cycle analysis of a cell proliferation associated human nuclear antigen defined by the monoclonal antibody Ki67. J. Immunol., *133:* 1710–1715, 1984.

27. Shi, S. R., Key, M. E., and Kalra, K. L. Antigen retrieval in formalin fixed, paraffin embedded tissues: an enhancement method for immuno-

histochemical staining based on microwave oven heating of tissue sections. J. Histochem. Cytochem., *39:* 741–748, 1991.

28. Emanuels, A., Hollema, H., and Koudstaal, J. Autoclave heating: an alternative method for microwaving? Eur. J. Morph., *32:* 337–340, 1994.

29. Jager, P. L., Luurtsema, G., Piers, D. A., Vries de, E. G. E, and Timmer-Bosscha, H. Characterisation of the uptake mechanism of L-3-[^{125}I]-iodo-α-methyl-tyrosine in GLC4 tumors cells: comparison with L-1-[^{14}C]-tyrosine. Eur. J. Nucl. Med., *26:* 972, 1999.

30. Deehan, B., Carnochan, P., Trivedi, M., and Tombs, A. Uptake and distribution of L-3-[^{123}I]iodo-α-methyl-tyrosine in experimental rat tumours: comparision with blood flow and growth rate. Eur. J. Nucl. Med., *20:* 101–106, 1993.

31. Garcia, J. R., Kim, E., Wong, F. C., Korkmaz, M., Yang, W. W., Yang, D. J., and Podoloff, D. A. Comparison of fluorine-18-FDG PET and technetium-99m-MIBI SPECT in evaluation of musculoskeletal sarcomas. J. Nucl. Med., *37:* 1476–1479, 1996.

32. Ramanna, L., Wasman, A., Binney, G., Wasman, S., Mirra, J., and Rosen, G. Thallium-201 scintigraphy in bone sarcoma: comparison with gallium-67 and technetium-99m-MDP in the evaluation of chemotherapeutic response. J. Nucl. Med., *31:* 567–572, 1990.

33. van Ginkel, R. J., Kole, A. C., Nieweg, O. E., Molenaar, W. M., Pruim, J., Schraffordt Koops, H., Vaalburg, W., and Hoekstra, H. J. L-[1–11C]-tyrosine PET to evaluate response to hyperthermic isolated limb perfusion for locally advanced soft-tissue sarcoma and skin cancer. J. Nucl. Med., *40:* 262–267, 1999.

34. Plaat, B. E. C, Kole, A. C., Mastik, M., Hoekstra, H. J., Molenaar W. M., and Vaalburg, W. Protein synthesis rate measured with L-[1–11C]tyrosine positron emission tomography correlates with mitotic activity and MIB-1 antibody-detected proliferation in human soft tissue sarcomas. Eur. J. Nucl. Med., *26:* 328–332, 1999.

35. Kuwert, T., Morgenroth, C., Woesler, B., Matheja, P., Palkovic, S., Vollet, B., Samnick, S., Maasjosthusmann, U., Lerch, H., Gildehaus, F. J., Wassmann, H., and Schober, O. Uptake of iodine-123-α-methyl-tyrosine by gliomas and non-neoplastic brain lesions. Eur. J. Nucl. Med., *23:* 1345–1353, 1996.

36. Woesler, B., Kuwert, T., Kurlemann, G., Morgenroth, C., Probst-Cousin, S., Lerch, H., Gullotta, F., Wassmann, H., and Schober, O. High amino acid uptake in a low-grade desmoplastic infantile ganglioglioma in a 14-year-old patient. Neurosurg. Rev., *21:* 31–35, 1998.

37. Kuwert, T., Probst-Cousin, S., Woesler, B., Morgenroth, C., Lerch, H., Matheja, P., Palkovic, S., Schafers, M., Wassmann, H., Gullotta, F., and Schober, O. Iodine-123-α-methyl tyrosine in gliomas: correlation with cellular density and proliferative activity. J. Nucl. Med., *38:* 1551–1555, 1997.

38. Dehdashti, F., Siegel, B. A., Griffeth, L. K., Fusselman, M. J., Trask, D. D., McGuire, A. H., and McGuire, D. J. Benign *versus* malignant intraosseous lesions: discrimination by means of PET with 2-[F-18]fluoro-2-deoxy-D-glucose. Radiology, *200:* 243–247, 1996.

39. Griffeth, L. K., Dehdashti, F., McGuire, D., Perry, D. J., Moerlein, S. M., and Siegel, B. A. PET evaluation of soft-tissue masses with fluorine-18-fluoro-2-deoxy-D-glucose. Radiology, *182:* 185–194, 1992.

40. Lodge, M. A., Lucas, J. D., Marsden, P. K., Cronin, B. F., O'Doherty, M. J., and Smith, M. A. A PET study of 18FDG uptake in soft tissue masses. Eur. J. Nucl. Med., *26:* 22–30, 1999.